International Journal of Innovative Computing, Information and Control
Volume **10**, Number **3**, June **2014**

ICIC International ©2014 ISSN 1349-4198
pp. 1189-1205

DEVELOPMENT OF A DRIVER INATTENTION DETECTION SYSTEM USING DYNAMIC RELATIONAL NETWORK

Md Rizal Othman[1,2], Zhong Zhang[1], Takuma Akiduki[1], Hajime Suzuki[1]
Takashi Imamura[1] and Tetsuo Miyake[1]

[1]Department of Mechanical Engineering
Toyohashi University of Technology
1-1 Hibarigaoka Tenpaku-cho, Toyohashi 441-8580, Japan
{ zhang; ima; miyake }@is.me.tut.ac.jp; mdrizal@ieee.org

[2]Faculty of Electrical and Electronic Engineering
University Malaysia of Pahang
Lebuhraya Tun Razak 26300 Kuantan, Pahang, Malaysia

Received June 2013; revised October 2013

Abstract. *In this study, a robust driver inattention detection system based on a driver model and dynamic relational network (DRN) using sensor data such as the quantity of vehicle speed and pedal operation is proposed. The system can be divided into three parts: the sensor diagnosis module, the driver model and inattentive driving detection. The sensor diagnosis module using the DRN is developed to analyze and identify faulty sensors (if any) through its measurement data. The driver inattention detection system was tested with actual data from a car driving on a highway and the system's diagnosis performance was evaluated. The results obtained indicate the effectiveness of the proposed system for inattentive driving detection.*
Keywords: Dynamic relational network, Sensor diagnosis, Intentional driving, Vehicle, Nonlinear auto regressive exogenous model

1. **Introduction.** The World Health Organization (WHO) reported that road accidents are a new form of global health threat. It has been estimated that every year more than 1.2 million people are killed, while 50 million others are injured as a result of road accidents [1]. The studies carried out to identify the leading cause of road accidents found that driver inattention is one of the main factors contributing to these accidents [1-5]. Miyaji et al. [6] reported in Japan that more than 25% of accidents are caused by drivers who lose concentration while driving a vehicle on the road. Furthermore, in 2006, the National Highway Traffic Safety Administration (NHTSA) stated that 80% of crashes and 65% of near-crashes were caused by inattentive driving. Generally, inattention can be defined as the withdrawal of attention due to the physical condition of the driver or external events, which can be divided into drowsiness and distraction. The problem becomes worse with the increasing variety of additional infotainment systems installed in vehicles that could cause drivers to be distracted [7, 8]. Therefore, the study of driver inattention is key to finding a solution to solve this problem or at least reducing the number of road accidents.

Numerous approaches and methods have been employed by the research community for monitoring and detecting driver inattention. Generally, the methods can be categorized into three groups: physiological measures [9-14], computer vision approaches [15-21] and driving performance measures [22, 23]. Physiological measures utilize biological signals such as the EOG, EEG, ECG, which are collected through electrodes contacting the human body. Then, signal processing methods are used to find the relationship between

these signals and the driver's state. Although these methods can provide more accurate results, they are impractical in real driving situations because they always require attachment of devices to the driver. The second approach using computer vision is more practical as it is non-intrusive to the driver, hence many active studies have been conducted in this field and a number of comprehensive methods have been created so far. Suzuki et al. [20] in their study detected eyelids using a neural network from the driver's facial image, which was captured by a camera placed in the car, and proposed a method to estimate driver alertness based on the movement of the eyelids. In reference [21] the authors proposed the use of Active Appearance Models to model the driver's face and extract seven characteristic points. Facial analysis was carried out using these characteristic points in order to detect driver drowsiness. Dinges and Perclos [15] proposed one of the most widely accepted metrics known as Percentage Eyelid Closure (PRECLOS) for the detection and evaluation of drowsiness using computer vision. In the third approach, researchers are interested in studying the effects of inattentive drivers on their driving performance. Similar to the computer vision approach, this approach also has the advantage of being non-intrusive to the driver compared with the first approach. Arnedt et al. [22] and A. Vakulin et al. [23] studied the relation between drowsiness and driving performance. However, only data from a simulated environment were used in the study because of the risks of placing drowsy drivers in real situations. Moreover, most of the studies described above only focus on detecting inattention caused by drowsiness and fatigue. Inattention caused by distraction (cognitive and visual) has been explored and discussed less.

On the other hand, Ishikawa et al. [24] proposed a method to detect driving with secondary tasks using driving behavior signals modeled with a Bayesian network, while taking driving situations into consideration. They showed that it is effective to consider driving situations when detecting distracted driving involving secondary tasks. Here the primary task is normal driving operation and secondary tasks such as talking on a cell phone, reading a road sign and searching for a song on the radio are imposed on the driver. However, the proposed method at best can achieve a correct detection rate of only 76%, so there is need for improvement. Kuroyanagi et al. [25], furthermore, analyzed hazardous situations in an actual driving environment based on the level of scene danger and driver response. They confirmed that driver response decreases when driving with secondary tasks. This shows that secondary tasks can be a good tool to create distraction for the driver during an actual driving task. In addition to a low detection rate, the proposed method uses the following distance (distance between cars) as one of the inputs to the model. Following distance is vulnerable to the external environment such as heavy rain and snow, which will cause the system capability to be reduced.

The authors [26, 27] proposed a new method to identify driver inattention due to cognitive distraction using a model-based technique. The method uses in-vehicle driving data collected by various sensors to predict output. Driver inattention is detected by analyzing the difference between the predicted and actual output, i.e., the residual of the model. The results demonstrated that the proposed method could differentiate and clearly distinguish between neutral and inattentive driving, but the detection rate dropped when one of the input sensors failed. Therefore, sensor failure diagnosis is needed in order to obtain an optimum detection rate and to avoid false alarms of the detection results.

Several studies have been done to detect and identify sensor failure. Li and Chen [28] proposed a linear model to model the process and thus the resultant residual is expressed in the form of a linear function. Simani et al. [29] used a linear state-space model to create a bank of observers and assumed only one sensor fault in the measurement process. Based on the residual generated, this method can identify a single faulty sensor.

However, many real processes including driver behavior are naturally nonlinear. Thus a linear model usually cannot hold the signal distribution well and the proposed methods can only give good predictions with some constraints. Nevertheless, a dynamic relational network (DRN) has been proposed as an effective technique for the abnormality diagnosis of the system with a large number of sensors [30, 31]. It can express a diagnosis object as an inequality limitation between variables in the observable condition when the diagnosis object is not expressed as a closed equation model. In addition, the DRN can perform the diagnosis that reflects the object when it cannot judge the object from a given sensor level exactly. Yamada and Ito [32] proposed a consistency diagnostic method of front vehicle recognition with the DRN using the data obtained by a laser radar and image sensor, and confirmed its effectiveness.

This study aims to develop a new robust system that can perform driver inattention detection. Here, the term 'robust' means that the system can still execute the detection process even when one of its inputs is absent (a faulty sensor). To progress towards this objective, this paper first constructs an in-vehicle sensor diagnosis module by DRN using the data from sensors, such as the vehicle speed and pedal operation. Then, a driver inattention detection system by combining the sensor diagnosis module and the driver model proposed by the authors [27] is introduced for the purpose of monitoring the state of the driver in the car and the detection of inattentive driving. The effectiveness of the proposed system is also evaluated in an actual car driving on an expressway using each operation data in the state that imposes a secondary task that causes inattentive driving and the state that does not impose a secondary task.

2. **Review of the Driving Model.** The authors [26, 27] have proposed a new driver-dependent model to capture nominal operation behavior of the driver. The study proved that current driver operation behavior can be represented as a function of the past and present driver behavior. Mathematically, this relation can be captured in a multivariable nonlinear autoregressive exogenous (NARX) network with the consideration of a time delay, order relations, a non-linearity between the time series data of driver operation from different sensors, as follows:

$$\begin{aligned}\hat{y}(t) =& f(u_1(t), u_1(t-1), \cdots, u_1(t-m), \cdots, u_n(t), u_n(t-1), \\ & \cdots, u_n(t-m), y_i(t-1), \cdots, y(t-m)),\end{aligned} \tag{1}$$

where $u(t)$ and $y(t)$ are the model inputs, $\hat{y}(t)$ is the estimated model output, $n+1$ is the number of inputs and m is the model time delay. In this study, there are three input signals ($n+1=3$), where $u_1(t)$ denotes the vehicle speed, $u_2(t)$ denotes the synthesis pedal pressure and $y(t)$ denotes the steering angle, respectively. The function $f(\cdot)$ is approximated by an NARX network. Figure 1 shows an example of the structure of the NARX network, where z^{-1} is operators of time delay. As can be seen in Figure 1, the proposed NARX network consists of three network layers which are the input layer, middle layer and output layer. Through Equations (2) and (3), the present value $\hat{y}(t)$ can be predicted from the input past chronological order data.

$$h_j = g_j\left(\sum_i^n w_{j,i}^1 v_i - \theta_j\right), \quad i = 1, 2, \cdots, n, \ \ j = 1, 2, \cdots, n_j, \tag{2}$$

$$V_o = g_o\left(\sum_{j=1}^{n_j} w_j^2 h_j - \theta_o\right), \quad j = 1, 2, \cdots, n_j. \tag{3}$$

where v_i is the ith network input, $w_{j,i}^1$ denotes the weight coefficient between the input and middle layers, w_j^2 is the weight coefficient between the middle and the output layers,

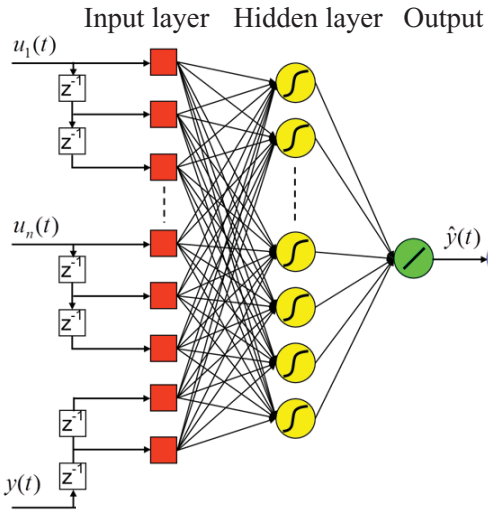

FIGURE 1. Driver model structure shown by the NARX network [27]

and θ_j and θ_o are the thresholds. In addition, $V_o = \hat{y}(t)$ is the output of the neural network at time t. Generally, the activated functions $g_j(\cdot)$ and $g_o(\cdot)$ express the input and output relations of the neuron, which often employ a function $g(z) = 1/(1 + e^{-z})$ called the sigmoid by a function with saturated values 0, 1. The weight coefficients and the thresholds are determined by operating repeatedly according to a learning rule using the Levenberg-Marquardt algorithm [34]. The predicted output value is obtained by inserting the series of past observation data into the network.

The ordinary (neutral) driving operation data of 15 licensed drivers were used for model fitting and validation. The model fitting was carried out through a learning process as described in reference [27]. Only driving operation data collected by normal sensors were used to develop and test the driver model. Then, the model was used to detect inattentive driving by analyzing the model residuals, i.e., the differences between the actual operation signal and the model-predicted driver actions. When a driver drives normally, the model residual has a small standard deviation and is in the form of white noise. However, when the driver model is used for data from driving with a secondary task, the standard deviation increased. To confirm the model effectiveness, the root mean square (RMS) value of the model residual was calculated using Equation (4) as below:

$$RMS = \sqrt{\frac{1}{m}\sum_{i=1}^{m}(e(t))^2}, \tag{4}$$

where $e(t) = \hat{y}(t) - y(t)$, $\hat{y}(t)$ is the model-predicted value at time t , $y(t)$ is the actual steering angle at time t and m is the number of data. Figure 2 shows the RMS value of the model residual in the cases of neutral driving (data details can be seen in Section 4.1) and inattentive driving for 15 licensed drivers [27]. As can be seen in Figure 2, in the case of neutral driving, the RMS values for fitting and validation are very small for all 15 drivers, which also indicate the effectiveness of the model. That is, the model can almost exactly predict the actual output value even though the difference data were used for these processes. Compared with this, in the case of inattentive driving, RMS values are almost more than two times larger than in the case of neutral driving. This is because the driver model cannot predict output well, so it produces a big residual. This also indicates the effectiveness of the model for inattentive driver detection.

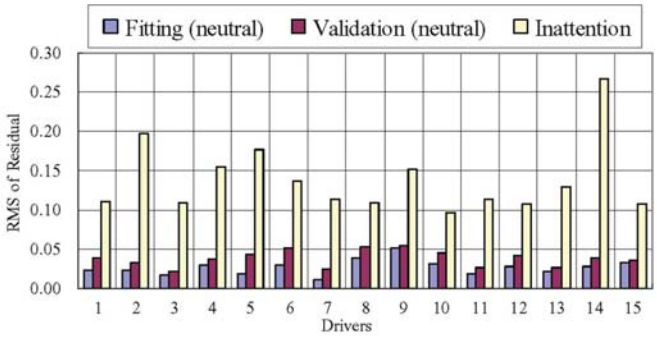

FIGURE 2. RMS values of neutral driving (fitting and validation process) and inattentive driving for 15 licensed drivers [27]

3. **A New Inattentive Driving Detection System Using a Dynamic Relational Network (DRN).** As is shown in Section 2, when data from inattentive driving are used, the driver model cannot predict output well, so it produces a big residual. However, if one of the sensors is damaged or not functioning properly, the proposed model also cannot provide good results, and sometimes it even gives the wrong detection result. This is because the model assumes that the driver is not driving in a normal condition due to wrong data collected by the faulty sensors. This situation can be avoided if we can exclude the faulty sensor's signal and only use the signal from the normal sensors as inputs into the detection system. Therefore, sensor failure diagnosis is needed in order to obtain an optimum detection rate and to avoid false alarm detection. In this section, a method of driving sensor diagnosis using the DRN will be discussed. Then a new inattentive driving detection system will be introduced.

3.1. **Principle and dynamics of the dynamic relational network (DRN).** In this section, the principle of the Dynamic Relational Network (DRN) is discussed. The DRN is a system consisting of different types of nodes that are linked together to form a network. One important feature of the DRN is that each node can evaluate other nodes or can be evaluated by other nodes independently and propagates its current state dynamically [30, 31]. This feature means the DRN can be used as a diagnostic system to detect faulty nodes.

Suppose that a measurement system consists of multiple heterogeneous nodes S_i, $(i = 1, 2, \cdots, m)$, tied together with a link to form a network. The diagnosis of whether the node is normal or faulty is carried out by determining the relationship of mutual trust between the nodes. The relationship between nodes S_i and S_j that are linked together is judged using measured values $x_i(t)$ and $x_j(t)$ of nodes S_i and S_j. If nodes S_i and S_j have maximum matchability, a test value, $T_{j,i}(t)$ is assigned to 1 $(T_{j,i}(t) = 1)$. On the other hand, if nodes S_i and S_j have no matchability, then $T_{j,i}(t) = -1$ is assigned. This process is performed between all linked nodes in the system. Figure 3 shows an example of the DRN with 5 nodes, where an arc labelled with 1 indicates that $T_{j,i}(t) = 1$ and -1 indicates that $T_{j,i}(t) = -1$.

The state of the node (normal or abnormal) cannot be determined by simply obtaining a test value for each node. However, which node is abnormal can be detected by including dynamics in this network [31], for example as expressed in Figure 4.

The diagnosis of the sensor as being normal or abnormal is carried out by the relationship of mutual trust between the sensors. Here, a count of an evaluation vote of the relationship of mutual trust from each sensor is performed and a change rate value $r_j(t)$

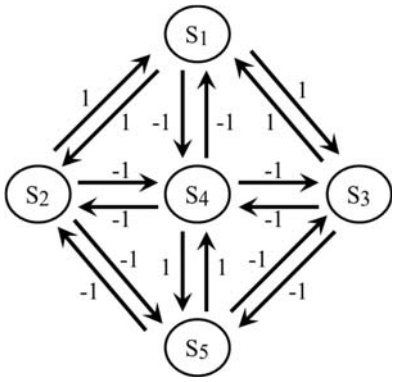

FIGURE 3. Derivation $T_{j,i}(t)$ for the network

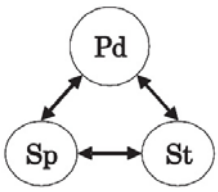

FIGURE 4. The DRN for excursively driving

at time t by a Skeptical model [33] expressed in the next equations is calculated.

$$\frac{dr_j(t)}{dt} = \sum_i T^+_{i,j}(t) R_i(t), \tag{5}$$

$$T^+_{i,j}(t) = T_{j,i}(t) + T_{i,j}(t) - 1, \tag{6}$$

$$R_j(t) = \frac{1}{1 + e^{-r_j(t)}}. \tag{7}$$

$$r_j(t) \in (\infty, +\infty),\ R_j(t) \in (0, 1)$$

where $R_j(t)$ represents the credibility or reliability of node S_j at time t, $r_j(t)$ is its intermediate variable and $T_{i,j}(t)$ is the test value obtained by S_i testing S_j. Initially, the reliability value $R(t)$ of all nodes at $t = 0$ is set to 1. Equations (5) and (6) are renewal equations for converging the network. Equation (7) is a sigmoid function and this network is known to converge. If $r_j(t)$ is large, $R_j(t)$ converges to 1. Otherwise, if $r_j(t)$ is small, $R_j(t)$ converges to 0. A node that ultimately has low reliability when the network has converged is determined to be abnormal.

3.2. **A new DRN structure for in-vehicle sensor diagnosis.** For the purpose of monitoring the condition of in-vehicle sensors that are used to collect driving data, the diagnosis algorithm is constructed based on the DRN's principle, where nodes in the DRN are replaced with an in-vehicle sensor. At first, the sensor network is constructed by connecting all the sensors to each other with virtual arcs. In this study, the relationship between each sensor is analyzed as follows and the DRN network is built.

Drivers always regulate speed by stepping on the accelerator pedal and the brake pedal and repeating this operation. Here the operation quantity of the accelerator pedal and the brake pedal, which are measured by different sensors, is treated as one pedal operation quantity because they are related to the adjustment of speed. The quantity of the accelerator pedal is defined as a positive value and the quantity of the brake pedal is defined as a negative value. Corresponding to this, the two sensors measuring the quantities of the

conventional accelerator pedal and brake pedal are treated as one virtual sensor. Based on the quantity of pedal operation and relation with the vehicle speed, the quantities of the pedal operation and vehicle speed are firstly tied with an arc.

Generally, a car often travels at more than 70[km/h] on an expressway. Even if the car is going straight, steering wheel operation is necessary for fine adjustment. In addition, if it is not going straight even if it is said to be going straight, the operation quite a few near cornering may be performed. In this case, it is thought that there is an action to decrease the vehicle speed, and to operate the steering wheel. Therefore, the steering angle and vehicle speed are tied by an arc.

As shown above, there is an operation action to decrease vehicle speed while driving and operating the steering wheel. It is necessary to regulate the quantity of pedal operation to decrease vehicle speed. In other words, it is thought that there is an action to operate the steering wheel by adjusting the quantity of pedal operation. Therefore, the quantity of pedal operation and the steering angle is tied by an arc.

Based on the above-mentioned argument, the three virtual sensors measuring the quantity of pedal operation, vehicle speed and steering angle are represented by three nodes of the DRN and the network is built. Figure 4 shows the built network for in-vehicle sensor diagnosis. The Pd in the figure shows the quantity of the pedal operation sensor, Sp the vehicle speed sensor, and St the steering angle sensor. Descriptions like these, hereafter, are used.

3.3. **Sensor diagnosis module with the in-vehicle sensor DRN.** This section will discuss a new sensor diagnosis module to identify sensor failure used in collecting driving data. Figure 5 shows the proposed sensor diagnosis module. As is shown in Figure 5, the sensor diagnosis module can be divided into two parts: offline sensor profiling and online sensor diagnosis. Offline sensor profiling part aims to extract the relationship between sensors that were tied together in a network. The relationship is obtained by calculating the proper parameter of normal data collected by the sensor. This step was performed offline and the parameter obtained will be used as a baseline or threshold value in the online sensor diagnosis part.

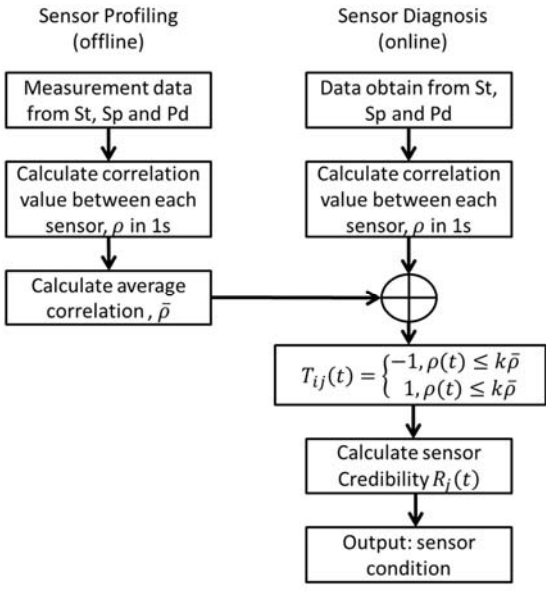

FIGURE 5. Sensor diagnosis module using the DRN

In this study, we use a correlation coefficient to represent the relationship between sensors tied in the network. Let S_i and S_j be two sensors connected together via an arc and $x_i(t)$ and $x_j(t)$ be measurement data from normal sensors S_i and S_j, respectively. The correlation coefficient is calculated at every tenth (10) sample data $x_i(t)$ and $x_j(t)$ using the following equation:

$$\rho_{ij}(\tau) = \frac{1}{m-1} \frac{\sum_1^m (x_i(t) - \bar{x}_i)(x_j(t) - \bar{x}_j)}{\sigma_{x_i} \sigma_{x_j}}, \tag{8}$$

where $\rho_{ij}(\tau)$ is the correlation coefficient, m is the number of samples in a window and $m = 10$, σ_{x_i} and σ_{x_j} are the standard deviations of data $x_i(t)$ and $x_j(t)$, and τ is the time of window center, respectively. Then, the baseline correlation coefficient $\bar{\rho}_{i,j}$ is obtained by averaging all correlation coefficients over M number of windows using the following equation:

$$\bar{\rho}_{ij} = \frac{\sum_1^M \rho_{i,j}(\tau)}{M}. \tag{9}$$

In the sensor diagnosis part, the current correlation coefficient, $\rho_{ij}(\tau)$ that is calculated using online measurement data $x_i(t)$ and $x_j(t)$ of sensors S_i and S_j is compared with the baseline correlation coefficient $\bar{\rho}_{i,j}$. When $\bar{\rho}_{i,j}$ deviates from the calculated $\rho_{i,j}(\tau)$ by a predetermine amount (called a threshold), the test node, $T_{i,j}(\tau)$ is decided as -1. In summary, the test node, $T_{i,j}(\tau)$ is decided based on the following rule:

$$T_{ij}(\tau) = \begin{cases} -1, & \rho_{i,j}(\tau) < k\bar{\rho}_{i,j} \\ 1, & \rho_{i,j}(\tau) \geq k\bar{\rho}_{i,j}, \end{cases} \tag{10}$$

where k is a constant value, $\bar{\rho}_{i,j}$ is the baseline correlation coefficient, $\rho_{i,j}(\tau)$ is the current correlation coefficient and $T_{i,j}(\tau)$ is a test node of the relationship of sensor S_i to sensor S_j. After the test node $T_{i,j}(\tau)$ of the correlation between sensor S_i and S_j has been decided, the credibility $R_j(\tau)$ of sensor S_j is calculated using expressions (5), (6) and (7).

3.4. **Driver inattention detection system using the driver model and the sensor diagnosis module.** In order to overcome the influence of faulty sensors on the detection rate of inattentive driving, a novel inattentive driving detection system based on the sensor diagnosis module and driver model is proposed. The idea is to eliminate the signal from a failed sensor before inattention detection is done by the driver models. By doing this, the signal from a faulty sensor will not affect the output of the driver models.

Figure 6 shows the overall concept of the inattentive driving detection system. As is shown in Figure 6, the system can be divided into three parts: the sensor diagnosis module shown in Figure 5 and Section 3.3, the driver model shown in Figure 1 and Section 2 and the inattention detection part. The sensor diagnosis module analyzes and identifies a faulty sensor (if any) through its measurement data. This module will produce total sensor credibility $R_o(t)$ that indicates the status of the input sensor of the system. $R_o(t)$ is obtained using the following expression:

$$R_o(t) = R_{St}(t) \left(\frac{2}{3} R_{Sp}(t) + \frac{1}{3} R_{Pd}(t) \right), \tag{11}$$

where R_{St} is the credibility of the steering sensor, R_{Pd} is the credibility of the pedal sensor and R_{Sp} is the credibility of the steering speed sensor. These credibility values indicate whether the respective sensor is working properly or not. The R_{St}, R_{Pd}, and R_{Sp} values were calculated individually using the sensor diagnosis module. Table 1 shows the interpretation of $R_o(t)$ and the sensor state. As can be seen in Table 1, Equation (11) is easily understandable since it gives a direct interpretation about the sensor's state.

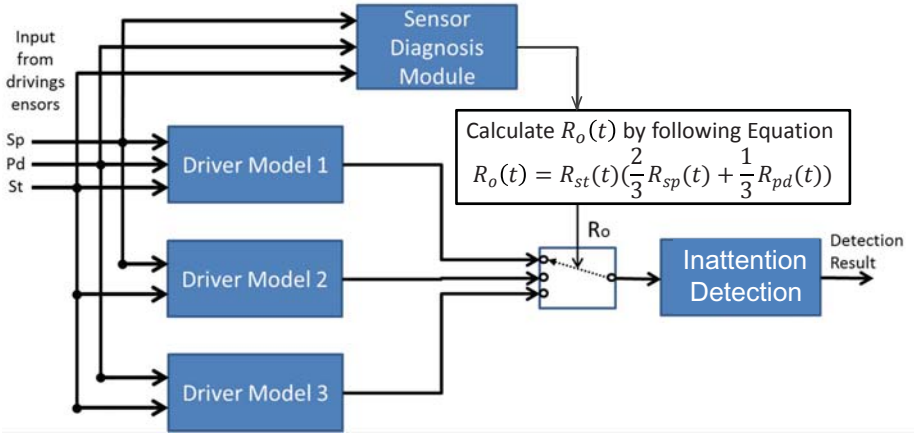

FIGURE 6. Inattentive driving detection system with DRN-based sensor diagnosis and driver model

TABLE 1. The interpretation of $R_o(t)$ and sensor state

R_o	Sensor State
1	All sensors are OK
2/3	Problem with pedal sensor
1/3	Problem with speed sensor
0	Problem with steering sensor

Therefore, $R_o(t)$ can be used as a selector to choose a suitable driver model for inattentive driving detection.

In the driver model part, three driver models were developed in the system. Driver model 1 is a normal model that has three input sensors shown in Section 2, while driver models 2 and 3 have only two input sensors. Based on (11) and Table 1, if all input sensors are normal, the output of the sensor diagnosis module is $R_o = 1$, so the output of driver model 1 is chosen. If a pedal sensor is diagnosed as having failed, in other words $R_o = 2/3$, the output of driver model 2 will be used to detect inattentive driving. The same concept is applied when $R_o = 1/3$, which means that the speed sensor is faulty, and then the output of driver model 3 will be used for the detection. However, if the total sensor credibility $R_o = 0$, where the steering sensor is the problem, then inattentive driving detection cannot be performed because the output of each model cannot be computed.

In addition, in the inattention detection part, the percentage of confidence score is calculated using the driver model residuals, which are obtained for the cases with and without a secondary task for all drivers, to inattentive driving detection. The percentage of confidence score is calculated based on the following equation:

$$C = 100e^{-R_{RMS}} \ [\%], \tag{12}$$

where C is the percentage of confidence score, $R_{RMS} = aRMS \times RMS$, RMS is calculated using Equation (4) and $a = 40$ is a constant value. Equation (12) shows that the percentage of confidence score depends on the residual's value. If the residual's value is small which shows that the driver is driving neutrally, the value of the confidence score, C will be high. In contrast, if the residual's value is big which shows that the driver is inattentively driving, the value of the confidence score, C will be low.

4. Confirmation Experiments and Results Discussion.

4.1. **Driving data.** The driving data utilized in this study were collected in collaboration with Professor Kazuya Takeda's Laboratory, Nagoya University, Japan. A real vehicle equipped with various sensors and cameras was used for synchronous recording of data, which consists of video, speech, driving control and physiological signals.

The aim of these experiments was to record multimodal driving data on different types of roads, such as city roads and expressways, under ordinary driving and with four tasks, in order to collect neutral and inattentive driving data. The four different secondary tasks are: 1) a navigation dialog task, 2) a repeating alphanumeric task, 3) a signboard-reading task and 4) a music retrieval task. Figure 7 shows the course map used in this study, where mark (1) denotes the start location, marks (2) to (7) and (12) to (13) denote city roads and marks (8) to (11) denote highway roads. Table 2 shows all twelve portions of the experiments that correspond to numbers (2) to (13) shown in Figure 7, the types of roads and their conditions during data collection.

TABLE 2. Description of experiments and driving conditions

Experi.	Road type	Task	Description
1	–	Idling	–
2	City	Ordinary driving	Driving without extra task
3	City	Signboard reading	Reading aloud information on signboard
4	City	Ordinary driving	Driving without extra task
5	City	Navigator	Following navigator instructions
6	City	Alphanumeric verbalization	Repeating four alphanumeric letters
7	City	Ordinary driving	Driving without extra task
8	Highway	Ordinary driving	Driving without extra task
9	Highway	Alphanumeric	Repeating four alphanumeric letters
10	Highway	Music retrieving	Music retrieving by spoken dialog
11	Highway	Ordinary driving	Driving without extra task
12	City	Music retrieving	Music retrieving by spoken dialog
13	City	Ordinary driving	Driving without extra task
14	–	Idling	–

FIGURE 7. The course map used in this study

On the city road, changes often occur outside of the car, such as pedestrians crossing and road traffic signals changing. Besides these, every car performs a variety of driving actions such as coming to a complete stop, turning left or right, and going slowly. In this study, in order to pay attention to the state of the driver, we want to remove elements such as the environment out of the car and the driving condition of the car if it is possible. Therefore, the driving data of the Highway are used. The operation signals of experiments 8, 11 (without secondary task) and 9 (with a secondary task of alphanumeric repeating), 10 (with a secondary task of music retrieval) from 20 licensed drivers were selected as examples, in order to investigate the influence of the secondary task on the driver's performance and to confirm the difference between inattentive driving and neutral driving. For the same reason, only the data when driving straight are treated.

An example of driving data that was measured from the operation signals in experiment 8 is shown in Figure 8, where the top figure shows the car speed, the bottom figure shows the steering angle and the middle figure shows the pedal pressure. The sampling rate of the operation signals is 100[Hz]. Note that the pedal pressure signal shown in the top figure is a synthetic signal, which was made to be the sum of the gas pedal pressure (made to be positive) and the brake pressure (made to be negative). In addition, in a part of the Highway, a secondary task such as alphanumeric repeating and music retrieval was assigned to the drivers, and driving without a task was defined as neutral driving and driving with a secondary task was defined as inattentive driving.

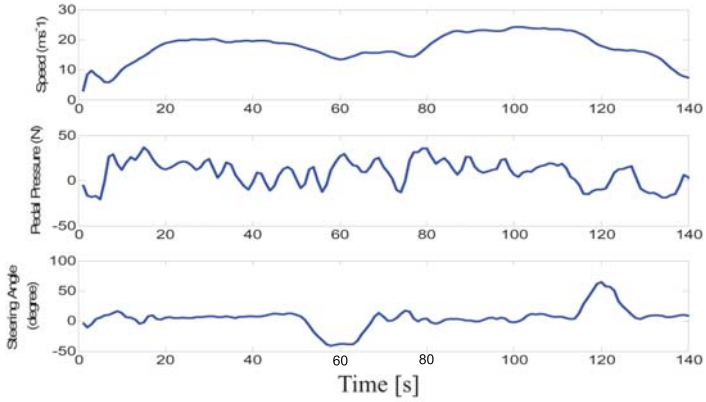

FIGURE 8. Example of neutral driving data of driver 18 in experiment 8

4.2. **Faulty sensor detection using the sensor diagnosis module.** There are many types of sensor failure, but here we consider a constant fault as an example because this type of failure occurs during the experiments and data collection. A constant fault happens when a sensor reports a constant value for a large number of successive samples. The reported constant value is either zero, very high, very low compared with the normal sensor reading and uncorrelated to the underlying physical phenomena. Examples of driving data with this type of sensor failure are shown in Figure 9, which is neutral driving data of driver 18 with a speed sensor failure. The top figure shows the pedal pressure, the bottom figure shows the steering angle and the middle figure shows the car speed.

Based on the method discussed in Section 3.3, faulty sensor diagnosis using the sensor diagnosis module can be realized. At first, offline analysis was performed to determine the average correlation (threshold) value, $\rho_{i,j}(\tau)$ of each driver by Equation (8) using all driving data from neutral and inattentive driving collected by the working sensor. The average correlation, $\bar{\rho}_{i,j}$ for each driver was calculated using Equation (9). Figure 10

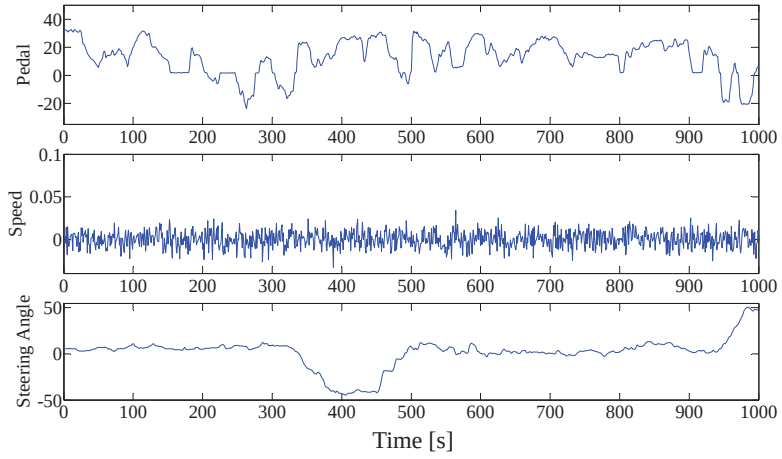

FIGURE 9. Example of neutral driving data of driver 18 with speed sensor failure in experiment 8

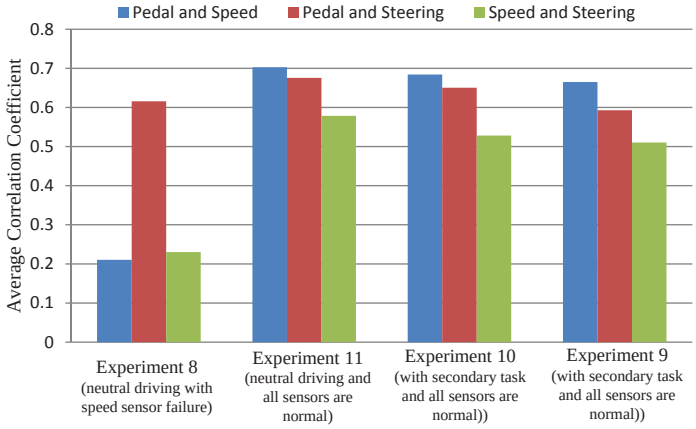

FIGURE 10. Average correlation coefficient from neutral driving, inattentive driving and neutral driving with sensor error

shows the average correlation coefficient for four experiments of driver 18. Experiment 8 is neutral driving with a speed sensor failure, experiment 11 is neutral driving, experiment 10 is driving with a music retrieval task and experiment 9 is driving with an alphanumeric repetition task. As can be seen in the figure, the average correlation between the pedal and speed, and speed and steering in the experiment 8 decreases due to the speed sensor failure.

After the threshold value (average correlation) $\bar{\rho}_{i,j}(\tau)$ for each driver has been determined, online in-vehicle sensor diagnosis can be performed. Measurement data from the speed sensor, pedal sensor and steering sensor are input into the sensor diagnosis module. Figure 11 shows an example of the diagnosis results of the sensor credibility using highway driving data shown in Figure 8 and Figure 12 shows an example of the diagnosis result of the sensor credibility using driving data on the highway shown in Figure 9. Figure (a) shows the $R_j(\tau)$ value of each sensor and (b) shows the sensor diagnosis module output. In Figure (a), the credibility, $R_j(\tau)$ is evaluated once every second and its magnitude is expressed in binary, either one or zero. In Figure (b), the sensor diagnosis module outputs a diagnosis result for each sensor every three seconds. This is because there is a possibility of momentary signal disorders caused by pebbles on the road. As can be seen in Figure 11(b), the sensor diagnosis module can provide good diagnosis results. The

sensor credibility of the speed, pedal and steering sensors converged to one for most of the time and indicates that the sensors were working properly. On the other hand, sensor credibility of the speed sensor shown in Figure 12(b) converged to zero and indicates the failure of the sensor. The results show the effectiveness of the proposed in-vehicle sensor diagnosis module. The same result can be obtained from other driving data.

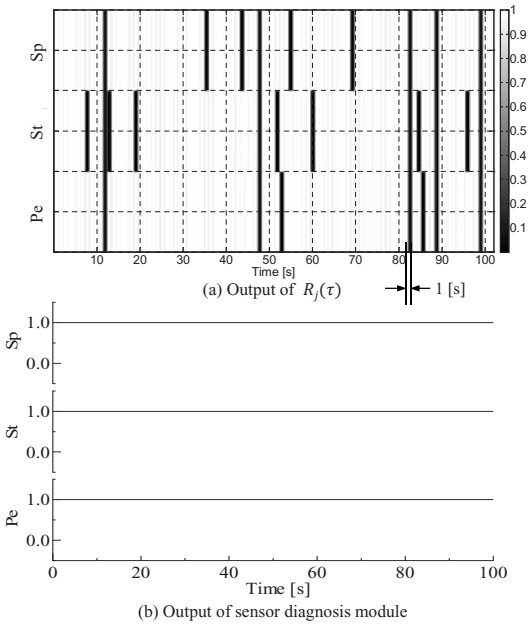

FIGURE 11. Example of sensor detected result obtained using the sensor diagnosis module in the case where all sensors are normal

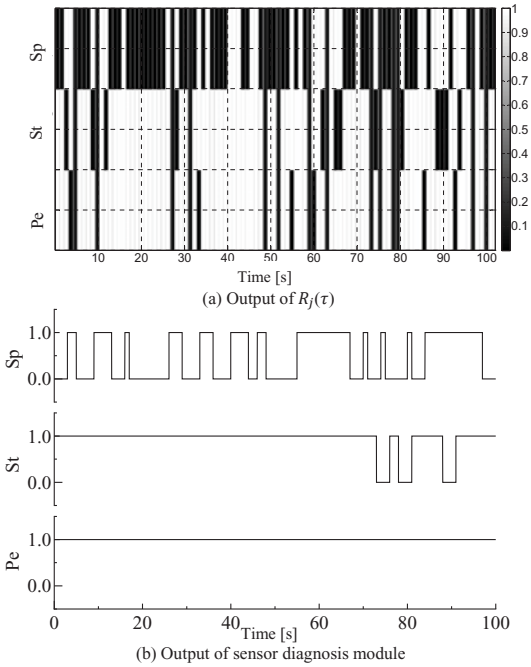

FIGURE 12. Example of sensor detected result obtained using the sensor diagnosis module in the case where the speed sensor is faulty

4.3. **Performance of driver inattention detection system.** In order to investigate the effect of sensor failure on the detection result and the effectiveness of this system, we first constructed and trained an individual driver model for 20 drivers. The model's construction and training procedures are the same as those discussed in Sections 2 and 3. We used neutral and inattentive driving data from the 20 drivers to test their model, respectively. All sensors (pedal sensor, speed sensor and steering angle sensor) were working properly when collecting driving data for drivers 1 to 15, while one of the sensors that measured data for drivers 16 to 20 was faulty. In other words, we used 15 driving data collected by normal sensors and 5 data collected by a faulty sensor (only one of the sensors was faulty) to study their effects on the detection result. The obtained results are very encouraging, which increased the detection rate and avoided false alarm detection. Figure 13 shows output from the driver models when inputting the neutral and inattentive driving data, where (a) is the output from the old driver model as discussed in Section 2 and (b) is the output from the new driver models shown in Section 3, which are in the driver model part of the inattentive driving detection system. As can be seen from Figure 13(a), using the old driver model, the RMS value increased dramatically if one of the sensors was faulty, and produced incorrect detections for drivers 16 to 20. However, with our new proposed driver models, the system can clearly identify neutral driving and inattentive driving even though there was a faulty sensor as shown in Figure 13(b). These results confirm the effectiveness of the proposed system.

Figure 14 shows the output of the driver inattention detection system, and the confidence score obtained by the inattention detection part from neutral driving (validation process) and inattentive driving data, where the confidence scores are calculated by Equation (12). As can be seen, the percentage of the confidence score is very high for all drivers and is more than 80[%] for the neutral operation residual whereas for inattentive operation the score drops below 70[%]. This result indicates the effectiveness of the proposed driver inattention detection system for inattentive driving detection and also shows that the percentage of the confidence score obtained from the inattention detection part can be used to interpret how much the driver is affected by distraction from the given task.

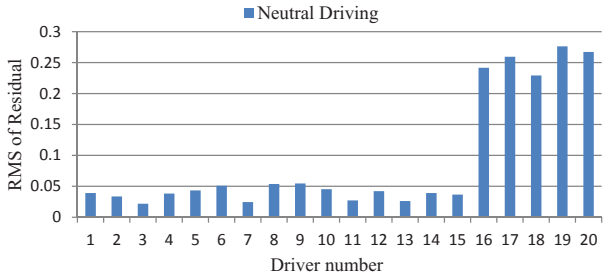

(a) Old model shown in Section 2.

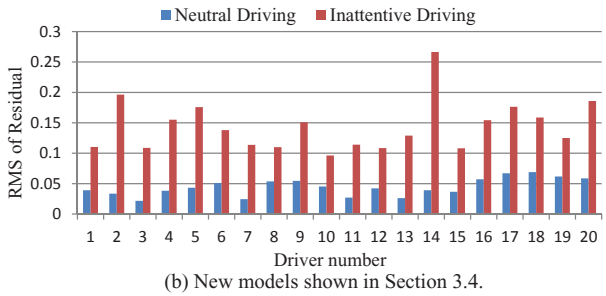

(b) New models shown in Section 3.4.

FIGURE 13. RMS of residual for neutral driving and inattentive driving data using two different methods

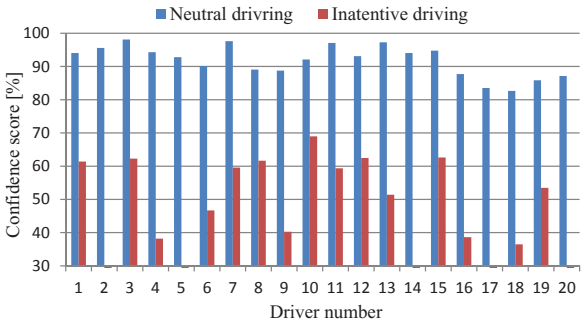

FIGURE 14. Output of the driver inattention detection system, where the confidence score was obtained by the inattention detection part from validation, testing and inattention driving data for the all drivers

Furthermore, the percentage of the confidence score differs for each driver. We think this is due to the fact that the influence of the secondary task for inattentive driving differs based on different driving experiences, and the driver's behavior.

5. **Conclusion and Remarks.** In this study, in order to monitor the driver's state in the car and to detect inattentive driving, a robust driver inattention detection system by driver model and dynamic relation network (DRN) using sensor data such as the quantity of vehicle speed and pedal operation was proposed. The system can be divided into three parts: the sensor diagnosis module, the driver model and inattention detection. In order to achieve robustness of the system, the sensor diagnosis module using the DRN was developed to analyze and identify faulty sensors (if any) through its measurement data. In the driver model part, three driver models were developed. Driver model 1 is a normal model that has three input sensors, while driver models 2 and 3 have only two input sensors. The built driver inattention detection system was operated with actual car driving data on a highway and the diagnosis performance was evaluated. As the obtained results, the percentage of the confidence score of system output was very high for all drivers and was more than 80[%] for the neutral operation residual whereas for inattentive operation the score dropped below 70[%]. This result indicates the effectiveness of the proposed driver inattention detection system for inattentive driving detection.

Future work will seek to determine which secondary tasks have the largest effect on driver inattention. Additionally, we intend to examine the influence of the secondary task on inattentive driving in different conditions of driving experience and driver behavior.

REFERENCES

[1] M. Peden, R. Scurfield, D. Sleet, D. Mohan, A. A. Hyder, E. Jarawan and C. Mathers, *World Report on Road Traffic Injury Prevention*, 3rd Edition, Geneva, 2004.

[2] E. D. Sussman, H. Bishop, B. Madnick and R. Walter, Driver inattention and highway safety, *Transp. Res. Rec.*, no.1047, pp.40-48, 1985.

[3] J. Wang, R. R. Knipling and M. J. Goodman, The role of driver inattention in crashes; new statistics from the 1995 crashworthiness data system (CDS), *Proc. of the 40th Annu.: Assoc. Advancement Automotive Med.*, pp.377-392, 1996.

[4] J. C. Stutts, D. W. Reinfurt, L. Staplin and E. A. Rodgman, The role of driver distraction in traffic crashes, *AAA Foundation of Traffic Safety*, 2001.

[5] European Project FP6 (IST-1-507674-IP), *AIDE – Adaptive Integrated Driver-Vehicle Interface*, http://www.aide-eu.org/index.html, 2004-2008.

[6] M. Miyaji, M. Danno and K. Oguri, Analysis of driver behavior based on traffic incidents for driver monitor systems, *IEEE Intelligent Vehicles Symposium*, pp.930-935, 2008.

[7] A. J. McKnight and A. S. McKnight, The effect of cellular phone use upon driver attention, *Accident Anal. Prev.*, vol.25, no.3, pp.259-265, 1993.
[8] D. L. Strayer and W. A. Johnston, Driven to distraction: Dual-task studies of simulated driving and conversing on a cellular telephone, *Psychol. Sci.*, vol.12, no.6, pp.462-466, 2001.
[9] B. T. Jap, S. Lal, P. Fischer and E. Bekiaris, Using EEG spectral components to assess algorithms for detecting fatigue, *Expert Systems with Applications*, vol.36, no 2, pp.2352-2359, 2009.
[10] I. Chouvarda, C. Papadelis et al., Non-linear analysis for the sleepy drivers problem, *MEDINFO*, vol.12, no.2, pp.1294-1298, 2007.
[11] M. V. M. Yeo, X. Li et al., Can SVM be used for automatic EEG detection of drowsiness during car driving? *Safety Science*, vol.47, no.1, pp.115-124, 2009.
[12] K. Q. Shen, X. P. Li et al., EEG-based mental fatigue measurement using multi-class support vector machines with confidence estimate, *Clinical Neurophysiology*, vol.119, pp.1524-1533, 2008.
[13] C. T. Lin and R. C. Wu, EEG-based drowsiness estimation for safety driving using independent component analysis, *Circuits and Systems I: Regular Papers*, vol.52, no.12, pp.2726-2738, 2005.
[14] C.-P. Chua, G. McDarby and C. Heneghan, Combined electrocardiogram and photoplethysmogram measurements as an indicator of objective sleepiness, *Physiological Measurement*, vo1.29, pp.857-868, 2008.
[15] D. Dinges and F. Perclos, A valid psychophysiological measure of alertness as assessed by psychomotor vigilance, *Tech. Rep., MCRT-98-006*, Federal Highway Administration, Office of Motor Carriers, 1998.
[16] M. Yang, D. Kriegman and N. Ahuja, Detecting paces in images: A survey, *IEEE Trans. on Pattern Anal. Machine Intell.*, vol.24, no.1, pp.34-58, 2002.
[17] Z. Zhu and Q. Ji, Real time 3D face pose tracking from an uncalibrated camera, *Proc. of CVPR Workshop*, pp.73-80, 2004.
[18] E. Murphy-Chutorian, A. Doshi and M. M. Trivedi, Head pose estimation for driver assistance systems: A robust algorithm and experimental evaluation, *Proc. of ITSC*, pp.709-714, 2007.
[19] N. Ikoma, Y. Miyahara and H. Maeda, Tracking of feature points in dynamic image with classification into objects and 3D reconstruction by particle filters, *Special Issue of International Journal of Innovative Computing, Information and Control on Fuzzy Systems and Innovational Computing*, vol.2, no.1, pp.167-180, 2006.
[20] M. Suzuki, N. Yamamoto, K. Yamada, O. Yamamoto, T. Nakano and S. Yamamoto, Presuming the driver's drowsiness by image processing and a trial of application to a driving support system, *IEEJ Trans. on Electronics, Information and System*, vol.126, no.12, pp.1497-1502, 2006.
[21] T. Kimura, K. Ishida and N. Ozaki, Possibility examination of sleepiness detection using expression features, *Transactions of Society of Automotive Engineers of Japan*, vol.39, no.2, pp.369-374, 2008.
[22] J. T. Arnedt, G. J. S. Wilde, P. W. Munt and A. W. Maclean, Simulated driving performance following prolonged wakefulness and alcohol consumption: Separate and combined contributions to impairment, *J. Sleep Res.*, vol.9, pp.233-241, 2000.
[23] A. Vakulin, S. D. Baulk, P. G. Catcheside, R. Anderson, C. J. van den Heuvel, S. Banks and R. D. McEvoy, Effect of moderate sleep deprivation and low-dose alcohol on driving simulator performance and perception in young men, *SLEEP*, vol.30, no.10, pp.1327-1333, 2007.
[24] H. Ishikawa, C. Miyajima, N. Kitaoka and K. Takeda, Detection of distracted driving using a Bayesian network, *ICIC Express Letters, Part B: Applications*, vol.2, no.2, pp.621-626, 2011.
[25] Y. Kuroyanagi, C. Miyajima, N. Kitaoka and K. Takeda, Analysis and detection of potentially hazardous driving situations, *ICIC Express Letters, Part B: Applications*, vol.2, no.2, pp.627-633, 2011.
[26] Md R. Othman, Z. Zhang, T. Imamura and T. Miyake, Driver inattention analysis using network based nonlinear ARX model, *ICIC Express letters, Part B: Applications*, vol.2, no.3, pp.679-686, 2011.
[27] Md R. Othman, Z. Zhang, T. Imamura and T. Miyake, A novel method for driver inattention detection using driver operation signals, *International Journal of Innovative Computing, Information and Control*, vol.8, no.4, pp.2625-2636, 2012.
[28] S. Li and Y. Chen, Sensor fault detection for manufacturing quality control, *MIE Department Rep., No. MIE-2006-01*, Univ. of Iowa, Iowa City, Iowa, 2006.
[29] S. Simani, C. Fantuzzi and S. Beghelli, Diagnosis techniques for sensor faults of industrial processes, *IEEE Trans. on Control Systems Technology*, vol.8, no.5, pp.848-855, 2000.
[30] Y. Ishida and F. Mizessyn, Sensor diagnosis of process plants by an immune-based model, *Transactions of Systems, Control and Information Engineers*, vol.7, no.1, pp.1-8, 1994.

[31] Y. Ishida and M. Tokumitsu, Adaptive sensing based on profiles for sensor systems, *Sensors*, no.9, pp.8422-8437, 2009.

[32] K. Yamada and T. Ito, An approach to understanding of driving environment using the network typed sensor fusion method, *IEICE Trans. of the Institute of Electronics, Information and Communication Engineers D-II*, Vol.J86-D-II, no.2, pp.223-232, 2003.

[33] C. Witteveen, Partial semantics for truth maintenance: A compositional approach, *Lecture Notes in Computer Science*, vol.478, pp.544-561, 1991.

[34] D. W. Marquardt, An algorithm for least squares estimation of nonlinear parameters, *SIAM J. Appl. Math.*, vol.11, pp.431-441, 1963.